

The error-floor of LDPC codes in the Laplacian channel

M. G. Stepanov^{1,2} and M. Chertkov¹

¹ *Complex Systems Group and Center for Nonlinear Studies, Theoretical Division,
Los Alamos National Laboratory, Los Alamos, NM 87545, USA*

² *Institute of Automation and Electrometry, Novosibirsk 630090, Russia
E-mails: stepanov@cnls.lanl.gov, chertkov@lanl.gov*

We analyze the performance of Low-Density-Parity-Check codes in the error-floor domain where the Signal-to-Noise-Ratio, s , is large, $s \gg 1$. We describe how the instanton method of theoretical physics, recently adapted to coding theory, solves the problem of characterizing the error-floor domain in the Laplacian channel. An example of the (155, 64, 20) LDPC code with four iterations (each iteration consisting of two semi-steps: from bits-to-checks and from checks-to-bits) of the min-sum decoding is discussed. A generalized computational tree analysis is devised to explain the rational structure of the leading instantons. The asymptotic for the symbol Bit-Error-Rate in the error-floor domain is comprised of individual instanton contributions, each estimated as $\sim \exp(-l_{\text{inst};L} \cdot s)$, where the effective distances, $l_{\text{inst};L}$, of the the leading instantons are 7.6, 8.0 and 8.0 respectively. (The Hamming distance of the code is 20.) The analysis shows that the instantons are distinctly different from the ones found for the same coding/decoding scheme performing over the Gaussian channel. We validate instanton results against direct simulations and offer an explanation for remarkable performance of the instanton approximation not only in the extremal, $s \rightarrow \infty$, limit but also at the moderate s values of practical interest.

A novel exciting era has begun in coding theory with the discovery of Low-Density-Parity-Check (LDPC) [1, 2] and turbo [3] codes. These codes are special, not only because they can approach the virtually error-free transmission limit, but mainly because a computationally efficient iterative decoding scheme is readily available. When operating at moderate noise values these approximate decoding algorithms show an unprecedented ability to correct errors, a remarkable feature that has attracted a lot of attention [4, 5, 6]. However, it was also shown that the approximate algorithms are incapable of matching the performance of Maximum-Likelihood (ML) decoding beyond the so-called error-floor threshold found at higher Signal-to-Noise-Ratios (SNR). The importance of error-floor, i.e. highest SNR, analysis was recognized in the early stages of the turbo code revolution [7], and it soon became apparent that LDPC codes are also not immune to the error-floor deficiency [4, 8]. To estimate the error-floor asymptotics in modern high-quality systems is a notoriously difficult task because direct numerical methods, e.g. Monte Carlo, cannot be used to determine Bit-Error-Rate (BER) below 10^{-9} . The main approaches to the error-floor analysis problem proposed to date include: (i) a heuristic approach of the importance sampling type [4], utilizing theoretical considerations developed for a typical randomly constructed LDPC code performing over the binary-erasure channel [9], and (ii) deriving lower bounds for BER [10].

Recently, we (in collaboration with V. Chernyak and B. Vasic) have also proposed a physics inspired approach that is capable of a computationally tractable analysis of the error floor phenomenon [11]. An efficient numerical scheme was proposed, which was ab-initio by construction, i.e. the optimization scheme required no additional assumptions (e.g. no sampling). This numerical optimization scheme, called the instanton-amoeba scheme, which plays a central role in our analysis, was shown to be accurate at producing configurations whose validity, for actual optimal noise configurations, can be verified theoretically. Finally, the instanton-amoeba scheme, introduced in [12], is also generic, in that there are no restrictions related to the type of decoding or the channel.

To illustrate the last, most important point, we complement the analysis of [11] that focused on the white Gaussian symmetric channel, by using the new results for the white Laplacian channel explained in this manuscript. Our choice of the Laplacian channel is arbitrary, e.g. influenced by its relevance to the description of fiber-optics communication channels. (Amplifier noise, known to have Gaussian statistics, contributes additively to the electric signal carrying the information. However, the intensity, the electric field squared, is detected on the receiver end. Therefore, the resulting transition probability, characterizing the noise in the fiber optics channel as the whole, shows exponential tails. See [15] for a discussion of these and other statistical errors in fiber optics channels.)

Our goal is to demonstrate using the example of the Laplacian channel that

- The numerical optimization approach to finding the most damaging configuration of the noise, instanton-amoeba, is computationally efficient.
- Subsequent theoretical analysis of the iterative decoding instanton based on the notion of the computational tree is channel specific, but it is also generalizable, i.e. the theoretical scheme can be modified to explain the rational structure of instantons for any, in particular Laplacian, channel.
- Instanton configurations for different channels are different. Thus, information on the error-floor analysis available for a channel (say, for the Gaussian channel) does not allow quantitative description of the error-floor in another channel (say, in the Laplacian channel).

This manuscript is organized as follows. We describe the problem of error-floor analysis, introduce the Laplacian channel and briefly review the results of [11] in Section I. Our theoretical analysis, generalizing the computational tree approach of [5], is detailed in Section II. Section III explains results of numerical instanton-amoeba evaluation. Here we present the three most important (for $s \gg 1$) instantons, for example of the min-sum decoding with four iterations performing over the $(155, 64, 20)$ LDPC code described in [14]. We also discuss here how the numerically found instanton is rationalized/explained theoretically. The comparison of Monte Carlo simulations and instanton prediction is discussed in Section IV. Some final remarks and comments are presented in Section V concluding the manuscript.

I. SETTING THE PROBLEM

Let us begin by introducing notation. A message word consisting of K bits is encoded in an N -bit long codeword, $N > K$. In the case of binary, linear coding a convenient representation of the code is given by $M \geq N - K$ constraints, often called parity checks or simply checks. Formally, $\boldsymbol{\sigma} = (\sigma_1, \dots, \sigma_N)$ with $\sigma_i = \pm 1$, is one of the 2^K codewords if and only if $\prod_{i \in \alpha} \sigma_i = 1$ for all checks $\alpha = 1, \dots, M$, where $i \in \alpha$ if the bit i contributes the check α . The relation between bits and checks (we use $i \in \alpha$ and $\alpha \ni i$ interchangeably) is often described in terms of the $M \times N$ parity-check matrix \hat{H} consisting of ones and zeros: $H_{\alpha i} = 1$ if $i \in \alpha$ and $H_{\alpha i} = 0$ otherwise. A bipartite graph representation of \hat{H} , with bits marked as circles, checks marked as squares, and edges corresponding to the respective nonzero elements of \hat{H} , is called the Tanner graph of the code. For an LDPC code \hat{H} is sparse, i.e. most of the entries are zeros. Transmitted through a noisy channel, a codeword gets corrupted due to the channel noise, so that the channel output is $\mathbf{x} \neq \boldsymbol{\sigma}$. Even though information about the original codeword is lost at the receiver, one still possesses the full probabilistic information about the channel, i.e. the conditional probability, $P(\mathbf{x}|\boldsymbol{\sigma}')$, for a codeword $\boldsymbol{\sigma}'$ to be a pre-image for the output word \mathbf{x} , is known. In the case of independent noise samples, the full conditional probability

can be decomposed into the product, $P(\mathbf{x}|\boldsymbol{\sigma}') = \prod_i p(x_i|\sigma'_i)$. A convenient characteristic of the channel output at a bit is the so-called log-likelihood, $h_i = \log[p(x_i|+1)/p(x_i|-1)]/2$. The decoding goal is to infer the original message from the received output, \mathbf{x} . ML decoding (which generally requires an exponentially large number, 2^K , of steps) corresponds to finding the most probable transmitted codeword given \mathbf{x} . Belief Propagation (BP) decoding [1, 2] constitutes a fast (linear in K, N) yet generally approximate alternative to ML. As shown in [1] the set of equations describing BP becomes exactly equivalent to the so-called symbol Maximum-A-Posteriori (MAP) decoding in the loop-free approximation (a similar construction in physics is known as the Bethe-tree approximation [16]), while in the low-noise limit, i.e. in the limit of very large SNR, $s \rightarrow \infty$, ML and MAP become indistinguishable and the BP algorithm reduces to the min-sum algorithm:

$$\eta_{i\alpha}^{(n+1)} = h_i + \sum_{\beta \neq \alpha} \prod_{j \in \beta} \text{sign}[\eta_{j\beta}^{(n)}] \min_{j \neq i} |\eta_{j\beta}^{(n)}|, \quad (1)$$

where the message field $\eta_{i\alpha}^{(n)}$ is defined on the edge that connects bit i and check α at the n -th step of the iterative procedure and $\eta_{i\alpha}^{(0)} \equiv 0$. The result of decoding is determined by a-posteriori log-likelihood, $m_i^{(n)}$, defined by the right-hand-side of Eq. (1) with the restriction $\beta \neq \alpha$ dropped. The BER measuring probability of errors at a given bit i becomes

$$B_i = \int d\mathbf{x} \theta(-m_i\{\mathbf{x}\}) P(\mathbf{x}|\mathbf{1}), \quad (2)$$

where $\theta(z) = 1$ if $z > 0$ and $\theta(z) = 0$ otherwise; $\boldsymbol{\sigma} = \mathbf{1}$ is assumed for the input (since in a symmetric channel the BER is invariant with respect to the choice of the input codeword). When the BER is small (SNR is large) the integral over output configurations \mathbf{x} in Eq. (2) is approximated by:

$$B_i \sim \sum_{\text{inst}} V_{\text{inst}} \times P(\mathbf{x}_{\text{inst}}|\mathbf{1}), \quad (3)$$

where \mathbf{x}_{inst} are the special instanton configurations of the output maximizing $P(\mathbf{x}|\mathbf{1})$ under the error-surface condition, $m_i\{\mathbf{x}\} = 0$; V_{inst} combines combinatorial and phase-volume factors (the latter one accounts for what physicists call fluctuations around the respective instanton). Individual instanton contributions into the rhs of Eq. (3) decrease significantly with increasing SNR. Thus at large SNR only instanton(s) with the highest $P(\mathbf{x}_{\text{inst}}|\mathbf{1})$ is (are) relevant.

For the common model of the Additive White Gaussian Noise (AWGN) channel,

$$p_G(x|\sigma) = \exp(-s^2(x - \sigma)^2/2) / \sqrt{2\pi/s^2}, \quad (4)$$

finding the instanton, $\boldsymbol{\xi}_{\text{inst}} = \mathbf{1} - \mathbf{x}_{\text{inst}} \equiv l(\mathbf{u})\mathbf{u}$, turns into minimizing the length $l(\mathbf{u})$ with respect to the unit vector in the noise space \mathbf{u} , where $l(\mathbf{u})$ measures the distance from the zero-noise point to the point on the error surface corresponding to \mathbf{u} . This task of the instanton analysis for the AWGN channel was discussed in detail in [11]. In [11] we developed a numerical scheme where the value of the length $l(\mathbf{u})$ for any given unit vector \mathbf{u} was found by the bisection method. The minimum of $l(\mathbf{u})$ was found by a downhill simplex method also called ‘‘amoeba’’ [13], with accurately tailored (for better convergence) annealing. (Note, that even previously, the numerical instanton method was successfully verified in [12] against analytical results in the loop-free case.) To demonstrate the utility of this method we chose in [11] the example of the (155, 64, 20) LDPC code of [14]. (The parity check matrix of the code is shown

in Fig. S1 of [11].) The code includes 155 bits and 93 checks. Each bit is connected to three checks while any check is connected to five bits. The minimal Hamming distance of the code is $l_{\text{ML};G}^2 = 20$, i.e. for $s \gg 1$, and if the decoding is ML, BER becomes $\sim \exp(-20 \cdot s^2/2)$ in the Gaussian channel. Iterative decoding is suboptimal, thus respective error-floor asymptotics become $P(\mathbf{x}_{\text{inst}}|\mathbf{1}) \sim \exp(-l_{\text{inst};G}^2 \cdot s^2/2)$. The numerical, and subsequent theoretical, analyses of [11] suggest that the instantons, as well as the respective effective distance, $l_{\text{inst};G}$, do depend on the number of iterations. Focusing primarily on the already nontrivial case of four iterations, we showed in [11] that the three minimal weight (largest probability) instantons have effective lengths, $l_{\text{a};G}^2 = 46^2/210 \approx 10.076$, $l_{\text{b};G}^2 = 806/79 \approx 10.203$ and $l_{\text{c};G}^2 = 44^2/188 \approx 10.298$ respectively. These instantons were found as the result of multiple attempts at instanton-amoeba minimization. The remarkable integer/rational structure of the instantons found numerically by instanton-amoeba for the AWGN channel admits a clear theoretical explanation discussed in details in [11]. We have already suggested in [11] that the instanton analysis (in both numerical and theoretical parts) is actually generic, and is thus applicable to wide range of different codes and channels.

To illustrate this last point we focus in this manuscript on analysis of the generalized Additive White Laplacian Noise (AWLN) channel:

$$p_{\text{GLap}}(x|\sigma) \propto \exp\left(-s\sqrt{(x-\sigma)^2 + \alpha^2}\right), \quad (5)$$

where s is the signal-to-noise-ratio (SNR) and α is the regularization parameter. (We are mainly interested in the $\alpha \rightarrow 0$, thus α is introduced primarily for the purpose of accurately regularizing/resolving the singularity at $\xi = x - \sigma = 0$.) If the detected signal at a bit is $1 - \xi$, the respective log-likelihood at the bit is defined as

$$h = \frac{1}{2s} \ln \left[\frac{p(\xi)}{p(2-\xi)} \right] = \frac{\sqrt{(2-\xi)^2 + \alpha^2} - \sqrt{\xi^2 + \alpha^2}}{2} \Big|_{\alpha \rightarrow 0} \rightarrow \begin{cases} -1, & \xi \geq 2; \\ 1 - \xi, & 2 \geq \xi \geq 0; \\ +1, & 0 \geq \xi. \end{cases} \quad (6)$$

where one chooses to measure log-likelihoods in the AWLN channel in units of SNR, s (and not in units of the SNR squared that was natural choice in the AWGN channel).

In the Laplacian channel ($\alpha = 0$), finding the instanton means to minimize $l(\mathbf{u}) \sum_i |u_i|$ with respect to the unit vector \mathbf{u} in the N -dimensional space, rather than minimizing $l(\mathbf{u})$ that was the case for the Gaussian channel. Notice, that just from this fact one finds absolutely no reason to expect that instantons for Gaussian and Laplacian channels are in any way related to each other. The contribution of an instanton to the BER for $s \gg 1$, characterized by the effective distance $l_{\text{inst};L}$, is estimated as $\sim \exp(-l_{\text{inst};L} \cdot s)$ in the case of the Laplacian channel.

II. GENERALIZED COMPUTATIONAL TREE ANALYSIS IN THE LAPLACIAN CHANNEL

In this Section we describe a theoretical approach to the instanton analysis. This analysis, based on the computational tree construction of Wiberg [5], was discussed in [11] for the Gaussian channel. Here we explain how the analysis can be modified to describe instantons in the case of the AWLN channel.

We start with the universal, i.e. channel insensitive, part of the construction. The computational tree is built by unwrapping the Tanner graph of a given code into a tree from a bit for which we would like to determine the probability of error. (This bit will be called erroneous bit.) The number of generations in the tree is equal to the number of min-sum iterations. As observed in [5], the result of decoding at the erroneous bit of the original code is exactly equal

to the decoding result in the tree center. It should be noted that once log-likelihoods representing an instanton are distributed on the tree, one can verify directly (by propagating messages from the leaves to the tree center) that the algorithm produces zero a-posteriori log-likelihood at the tree center. Any check node processes messages coming from the tree periphery in the following way: (i) the message with the smallest absolute value (one assumes no degeneracy) is passed, (ii) the source bit of the smallest message is “colored”, and (iii) the sign of the product of inputs is assigned to the outcome. At any bit that lies on the colored leaves-to-center path the incoming messages are summed up. The initial messages at any bit of the tree are log-likelihoods and, therefore, the result obtained in the tree center is a linear combination of the log-likelihoods with integer coefficients. The integer n_i corresponding to bit i of the original graph is the sum of the signatures over all colored replicas of i on the computational tree. Therefore the condition at the tree center becomes $\sum_i n_i h_i = 0$.

So far the discussion has been generic. Let us now adapt this generic construction to the case of the generalized AWLN channel described by Eq. (5). Returning from the computational tree to the original graph and maximizing the integrand of Eq. (2) with the condition, $\sum_i n_i h_i = 0$, enforced we arrive at the following expressions for the effective length:

$$l_{\text{inst};L} = \sum_i \sqrt{\xi_i^2 + \alpha^2} + \lambda \sum_i n_i h_i, \quad (7)$$

where λ is the Lagrange multiplier enforcing the zero a-posteriori log-likelihood condition at the tree center. Minimizing Eq. (7) with respect to ξ_i one derives

$$\frac{\xi_i}{2 - \xi_i} \sqrt{\frac{(2 - \xi_i)^2 + \alpha^2}{\xi_i^2 + \alpha^2}} = \frac{\lambda n_i}{2 - \lambda n_i}. \quad (8)$$

Expressing ξ_i in terms of n_i and λ involves solving a cubic equation. Note also that, first, the left-hand-side of Eq. (8) is monotone with respect to ξ_i in the interval of $0 \leq \xi_i < 2$, and, second, the expression becomes 1 as $\alpha \rightarrow 0$. Consider the domain of $2 > \xi_i \geq 0$ and $\alpha \ll (2 - \xi_i)$. Then Eq. (8) becomes

$$\xi_i \approx \frac{\alpha \lambda n_i}{2\sqrt{1 - \lambda n_i}}, \quad h_i \approx 1 - \frac{\xi_i}{\lambda n_i} \approx 1 - \frac{\alpha}{2\sqrt{1 - \lambda n_i}}. \quad (9)$$

One observes that either of the two possibilities is realized at $\alpha \rightarrow 0$: (1) $\lambda n_i \rightarrow 1$ and $\xi_i \rightarrow \text{const} \neq 0$; or (2) $\lambda n_i \rightarrow \text{const} \neq 1$ then $\xi_i \rightarrow 0$. One should also add to these two possible cases a third one (that is obviously not explained by Eq. (9)) where ξ lies exactly on the border of the monotone interval, i.e. at $\xi = 2$ and $h = -1$.

One finds that structurally an instanton consists of three types of colored bits corresponding to $\xi = 0$, $0 < \xi < 2$ and $\xi = 2$ respectively. One also finds that for all the colored bits with $0 < \xi < 2$ all the respective n_i approach the same limit, $n_i \rightarrow 1/\lambda$, even though respective ξ_i may be distinct. This results in the following form of the zero a-posteriori log-likelihood condition at the tree center

$$\sum_i n_i h_i = N_c - n_* \sum_{i \in \text{set}} \xi_i - 2N_2 = 0, \quad l_{\text{inst};L} = 2m_2 + \sum_{i \in \text{set}} |\xi_i| = \frac{N_c - 2N_2}{n_*} + 2m_2, \quad (10)$$

where “set” is the set of colored bits on the original graph with $0 < \xi_i < 2$; N_c is the total number of the colored bits on the computational tree; N_2 is the number of marginal, $\xi = 2$, bits on the computational tree; n_* is the number of replicas found on the computational tree for a bit i that belongs to the set (this is the same number for all $i \in \text{set}$); m_2 is the number of distinct marginal (i.e. $\xi = 2$) bits on the original graph.

Eq. (10) represents the major theoretical result of our analysis. It explains the rational origin of the effective length and shows how the effective length depends on the set of integers, N_*, N_2, n_* and m_2 carrying the coding/decoding specific information. Notice also a remarkable common feature of the instantons. There is actually a strong degeneracy here if the number of colored bits with $0 < \xi < 2$ is two or larger: the effective length depends only on $\sum_{i \in \text{set}} \xi_i$, while otherwise, and modulo the requirement $0 < \xi_i < 2$, the ξ_i fields can be chosen arbitrarily. Therefore, to estimate the BER corresponding to the given set of integers, N_c, N_2, n_*, m_2 , thus explaining a continuous family of instantons rather than an individual instanton, one should also account for the degree of degeneracy (volume of the respective part of the phase space), $B \sim V(N_c, N_2, n_*, m_2) \times \exp[-s \cdot l_{\text{inst};L}]$. Our estimate shows that the $V(N_c, N_2, n_*, m_2)$ -terms give sub-leading (i.e. non-exponential in s) corrections to the major (effective length) factors.

III. INSTANTON-AMOEBAS CALCULATIONS IN LAPLACIAN CHANNEL

So far we have not discussed how to find the discrete values N_c, N_2, n_* and m_2 that are obviously dependent on the explicit structure of the LDPC code considered. To solve this problem we adopt the instanton-amoeba approach of [11].

We consider the (155, 64, 20) LDPC code of [14] as an example. The minimal Hamming distance of the code is $l_{\text{inst};L} = 20$, i.e. for $s \gg 1$, and if the decoding is ML, the BER becomes $\sim \exp(-20 \cdot s)$ in the case of the Laplacian channel. The BER is higher, $\sim \exp(-l_{\text{inst};L} \cdot s)$ with $l_{\text{inst};L} < 20$, if one decodes iteratively. For the min-sum decoding with 4 iterations we found that three minimal length instantons are characterized by $l_{a;L} = 7.6$, $l_{b;L} = 8$ and $l_{c;L} = 8$ respectively. These instantons were disclosed as the result of multiple attempts at instanton-amoeba numerical minimization described above.

The colored parts of the Tanner graph of the code and the respective parts of the computational tree for the three configurations are shown in Fig. 1: the three panels (a,b,c) correspond to the three instantons showing minimal effective lengths. Each panel consists of two diagrams showing the relevant (colored) part of the Tanner graph and respective (four iterations deep) part of the computational tree. Bits/circles are shown with numbers correspondent to the ordering of the bits explained in [11]. The shadow bit is the erroneous one, i.e. it is the bit whose a-posteriori log-likelihood is exactly zero on the 4 step of the min-sum decoding. According to our theoretical analysis detailed above (that is also confirmed numerically in detail) there are three types of colored bits/circles with $\xi = 0$, $0 < \xi < 2$ and $\xi = 2$, shown in Fig. 1 in white, green and red respectively. The white bits on the computational tree that are not numbered (and respective bits of the Tanner graph simply not shown in the Figure) can be chosen arbitrarily with the only requirement that they are distinct from any bits shown numbered in the Figure.

Configuration (a) shown in Fig. 1a consists of 2 green bits with $0 < \xi < 2$ (numbers 79 and 89) each appearing 5 times on the computational tree, and 2 red bits with $\xi = 2$ (numbers 24 and 151) each appearing 7 times on the computational tree. The remaining 151 bits carry $\xi = 0$ noise. Therefore, the respective integers corresponding to this instanton are $N_c = 46$, $N_2 = 2 \cdot 7 = 14$, $n_* = 5$, $m_2 = 2$, thus resulting according to Eq. (10) in $l_{a;L} = 7.6$. This effective distance was found with numerical precision by the instanton-amoeba method. The degeneracy in this family of instantons is one parametric: $h_3 + h_{16} = -8/5$ and $-1 \leq h_3, h_{16} \leq 1$. Here, the erroneous bit, i.e. the bit with zero a-posteriori log-likelihood (marked striped in the Fig. 1a) is the white one.

Configuration (b) consists of three green bits, with $0 < \xi < 2$, appearing four times each on the computational tree, and three red bits, with $\xi = 2$, appearing 7, 6 and 6 times respectively. For this instanton one finds, $N_2 = 19$, $n_* = 4$, and $m_2 = 3$ (N_c is always 46 for the four iterations decoder) so that $l_{b;L} = (46 - 2 \cdot 19)/4 + 2 \cdot 3 = 8$. The erroneous bit (number 139) is white. One bit, numbered 112, is special here. Even though this bit has many replicas on the computational

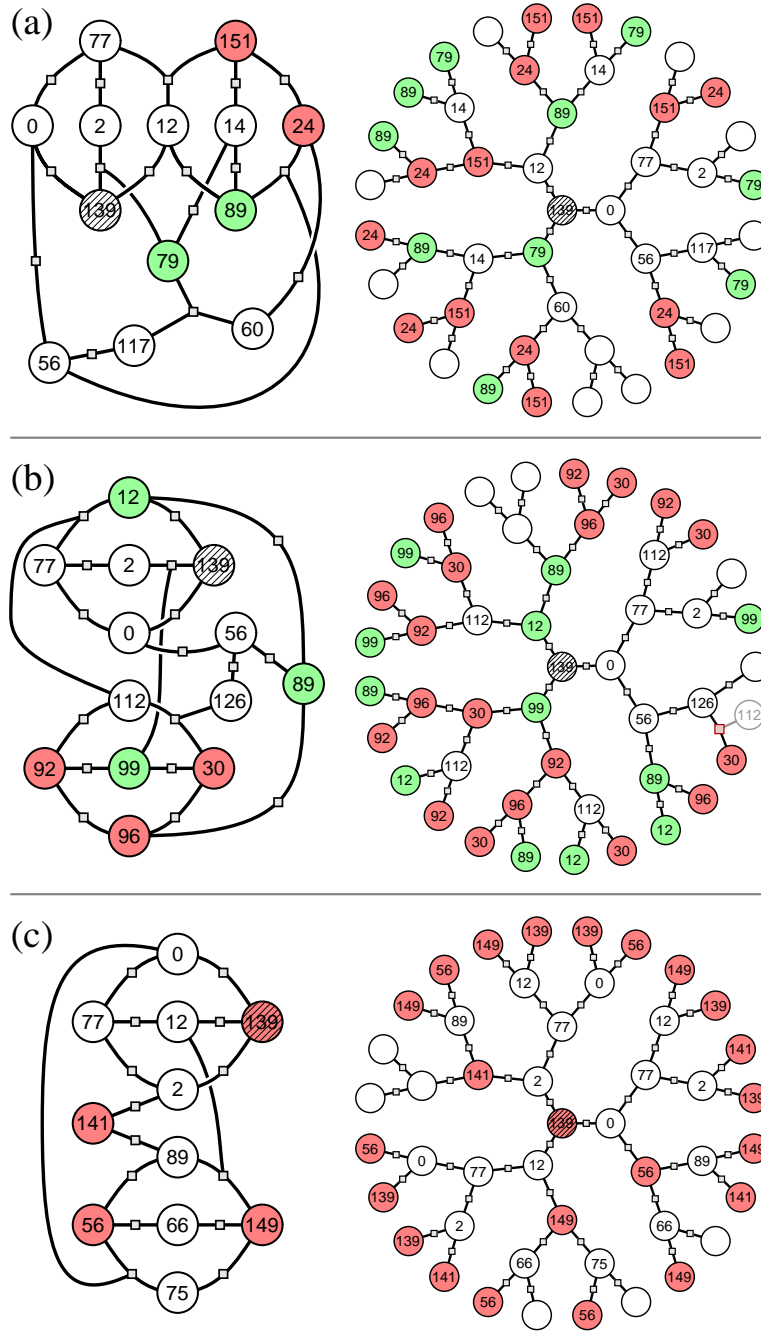


FIG. 1: Visualization of three instantons with shortest effective lengths found by the instanton-amoeba scheme. Only relevant parts of the Tanner graph for the $(155, 64, 20)$ code and respective computational tree with four iterations are shown. Numbers marking the bits are introduced in accordance with the convention described in [11]. The color coding used for bits is white for $\xi = 0$, green for $0 < \xi < 2$ and red for $\xi = 2$. See detailed explanations in the text.

tree, thus potentially, it would be advantageous to have it green carrying the non-zero value of the noise, self-consistency strictly requires that $\xi_{112} = 0$. There are at least two reasons for this. First of all, if bit 112 turns green making $\xi_{112} \neq 0$ one of its replicas on the computational tree (the one marked pale and adjusted to the red check/square in Fig. 1b) screens bit 30 (positioned next to the red check) in the sense that this screened bit will not contribute to n_{30} . Consequently, n_{30} becomes 6 and not 7, thus making N_2 smaller and $l_{\text{inst:L}}$ larger. Second, if $\xi_{112} \neq 0$ then one of the 5 replicas of the bit 112 contributes a-posteriori log-likelihood at the tree center

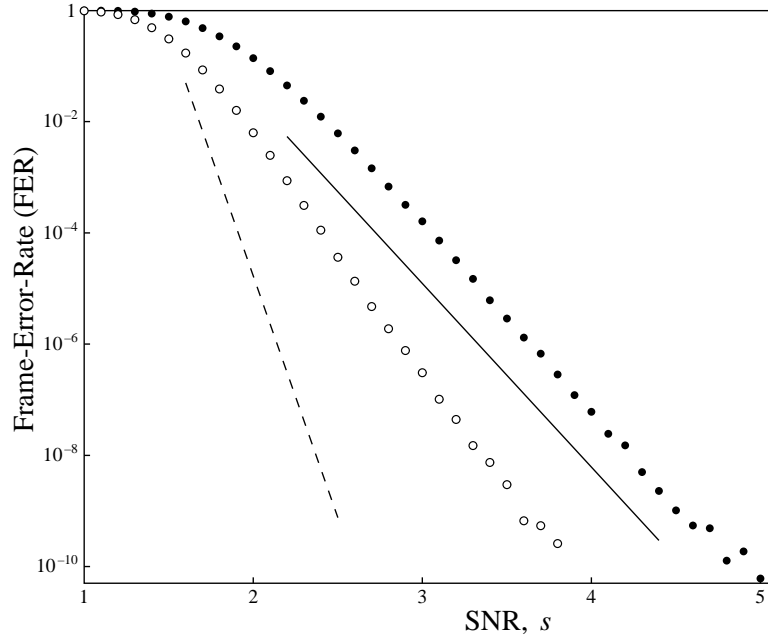


FIG. 2: Frame-Error-Rate vs Signal-to-Noise ratio, s , for the $(155, 64, 20)$ code with four iterations of the min-sum decoding over the Laplacian channel. Solid and dashed lines show slopes (defined upto a constant shift in the log-lin plot) correspondent to the instanton with the shortest effective distance, $l_{a;L} = 7.6$, and to the ideal ML decoding with the Hamming distance, $l_{ML;L} = 20$, respectively. Filled and empty circles show results of direct Monte-Carlo simulations for 4 and 1024 iterations respectively.

with “-” sign and n_{112} becomes equal to 3, rather than 5. This number is smaller than $n_* = 4$ thus leading to the undesired effective length increase. Finally, the resulting degeneracy in the instanton family is two-parametric (corresponding to appearance of three, and not four, green bits): $h_{12} + h_{89} + h_{99} = 1$ and $-1 \leq h_{12}, h_{89}, h_{99} \leq 1$.

Configuration (c) has the same effective length as configuration (b), $l_{c;L} = 8$, even though it is very different structurally. The (c) instanton has no green bits, thus it is non-degenerate and only one special configuration of h_i fields is realized. There are four red bits, 56, 139, 141 and 149, appearing on the computational tree 6, 7, 4 and 6 times respectively. The erroneous bit, 139, is red. The integers are $m_2 = 4$, $N_2 = 23$ and $N_c - 2N_2 = 0$, thus according to Eq. (10) $l_{c;L} = 2m_2 = 8$.

In [11] we have argued, following the logic of [5], that each instanton is equidistant from some number of pseudo-codewords, i.e. codewords on the respective computational tree. This observation is obviously generic and thus it is applicable as well to the case of the Laplacian channel considered in the manuscript. For any of the instantons discussed above and illustrated in Fig. 1 there exists a respective pair of pseudo-codewords. (As argued in [5] an instanton may be degenerate — corresponding to a triple or in principle to even larger set of pseudo-codewords. This degeneracy, that was found present in the AWGN channel, was not observed here for the AWLN channel.) The first pseudo-codeword in a pair is just the all +1 codeword (+1 sits at every bit). The second pseudo-codeword in a pair can be introduced according to the following rule: put -1 at any colored (i.e. white, green or red) bit and +1 at any uncolored (thus not shown in Fig. 1) bits. Obviously this choice of the pseudo-codewords pairs is unambiguous. Indeed the white bits that are not numbered can be chosen arbitrarily (within appropriate bounds described above). Moreover, the ambiguity in choosing the second pseudo-codeword (containing -1 bits) is even stronger. Indeed, this second pseudo-codeword can consists only of two -1 bits (all other bits will carry +1): one -1 should be positioned at

any red bit (with $\xi = 2$) from the last generation of the computational tree and another -1 is placed on any uncolored bit sharing a check with the red bit. This special form of degeneracy is due to the fact that log-likelihoods assigned to any red bit and to an uncolored bit adjusted to the red one are the same in absolute value but opposite in sign.

IV. VALIDITY OF INSTANTON APPROXIMATION AT MODERATE SNR

The analysis of the previous Section suggests that the leading $s \rightarrow \infty$ asymptotic for BER (and for the Frame-Error-Rate as well) is governed by the instanton with the lowest effective length found, i.e. $B \sim \exp[-s \cdot l_{a;L}]$. We have checked this prediction against direct Monte-Carlo (MC) simulations and found very good agreement already in the range accessible for the MC, $B \lesssim 10^{-9}$. See Fig. 2. We observed that the actual behavior of BER is well described by the instanton not only in the asymptotic regime of highest SNR but also in the regime of moderate SNR where there is no a-priori reason to expect the instanton approximation to work so well. Our further discussion is to eliminate this point suggesting a plausible explanation for this surprising generality of the instanton asymptotic.

Let us first clarify why the validity of the instanton asymptotic at the moderate values of SNR shown in Fig. 2 is surprising. Indeed, according to Eq. (5) the average value of the noise configuration length, $l = \sum_i |\xi_i|$, unconstrained by the requirement to have zero a-posteriori log-likelihood at a bit, is $\langle l \rangle \sim N/s$. This means that even at $s = 5$ (the largest SNR shown in Fig. 2), where the error probability is already small, $FER \sim 10^{-10}$, the typical length of noise realization is still essentially larger than the respective instanton prediction: $l \sim 155/5 = 31 > l_{a;L} = 7.6$. Therefore, naively one expects the instanton to work well at $s \gtrsim 20$, where $\langle l \rangle \lesssim l_{a;L}$, while according to the MC results shown in Fig. 2 the instanton asymptotic sets already at $s \simeq 2.5$, where $FER \sim 10^{-2}$. (Notice, that the situation for the Gaussian channel is similar, see Fig. S2 of [11]. There the typical $l^2 \sum_i \xi_i^2$ is $\sim N/s^2$, resulting in $\langle l^2 \rangle \approx 30$, while the respective instanton value is $l_a^2 \approx 10.076$.)

Our approach to explaining the validity of the instanton asymptotic already at the moderate SNR is of the reverse engineering type: we first formalize what the Monte-Carlo results suggest and then present a plausible explanation for this phenomenon.

One useful object is the probability distribution function of the channel noise length (fully unconstrained), that gets the following forms for the Gaussian and Laplacian channels respectively: $\mathcal{P}_L(l) = s^N l^{N-1} [\Gamma(N)]^{-1} \exp(-l \cdot s)$ and $\mathcal{P}_G(l) = s^N l^{N-1} 2^{1-N/2} [\Gamma(N/2)]^{-1} \exp(-l^2 \cdot s^2/2)$. Typical noise configuration forms a “spherical” layer with “radius” $l = \sum_i |\xi_i| \approx N/s$ in the N -dimensional noise space (or $l^2 = \sum_i \xi_i^2 \approx N/s^2$ for the Gaussian channel). The “spherical” layer becomes thinner as N grows. Obviously $\mathcal{P}(l)$ does depend on the channel but it does not depend on the decoding scheme. Another useful object, that is decoding sensitive, is the (cumulative) distribution function $\mathcal{F}_{ES}(l)$ of the length for the points positioned exactly at the error-surface. Estimation for FER is related to the area of spherical layer that lies outside of the error surface: $FER = \int dl \mathcal{P}(l) \mathcal{F}_{ES}(l)$. Strictly speaking this relation is exact for the Gaussian channel, but it is only qualitatively right (up to a $O(1)$ coefficient accounting accurately for the phase factor) in the Laplacian channel case. The integral $FER = \int dl \mathcal{P}(l) \mathcal{F}_{ES}(l)$ can be viewed as the Laplace transform. Deducing from the Monte Carlo simulations that the instanton asymptotic is valid, $FER \propto \exp(-l_{inst;L} \cdot s)$ (or $FER \propto \exp(-l_{inst;G}^2 \cdot s^2/2)$ for the Gaussian channel) one derives by the inverse Laplace transform $\mathcal{F}_{ES}(l) = (1 - l_{inst;L}/l)^{N-1}$ (or $\mathcal{F}_{ES}(l) = (1 - l_{inst;G}^2/l^2)^{N/2-1}$ for the Gaussian channel).

We suggest that the special dependence of \mathcal{F}_{ES} on l , deduced from the MC simulations, corresponds to an $(N-1)$ -dimensional area of the part of error-surface with lengths l or less, $\mathcal{F}_{ES} \sim \delta^{N-1}$, where δ is the respective line element. Given that the instanton configuration is

extremal one assumes that, $l - l_{\text{inst}} \propto \delta^2$, that results exactly in the right expression for $\mathcal{F}_{\text{ES}}(l)$ in the Gaussian channel. We ought to assume that in the Laplacian channel case expansion of l with respect to $\delta \ll l$ about $l \sim l_{\text{inst}}$, is of another type, $l - l_{\text{inst}} \propto \delta$, thus confirming the $\mathcal{F}_{\text{ES}}(l)$ dependence on l observed in the Laplacian channel simulations.

V. CONCLUSIONS

The set of tasks formulated in the introductory Section was accomplished in Sections II-III. We have shown for the example of the Laplacian channel that the instanton-amoeba optimization scheme, introduced in [12] and tested in [11] for the Gaussian channel, is computationally efficient. We extended the theoretical analysis of [11], based on the computational tree approach of [5], explaining the rational structure of instantons in the Laplacian channel. The instantons are shown to be different for different channels considered with the same coding/decoding scheme. Even though the fact that effective lengths differ for different channels was already demonstrated in [6] for the example of the binary symmetric and binary erasure channels, this manuscript additionally proved that not only the effective weights but also the instanton configurations themselves were different structurally for different channels.

We conclude by noting that the observations made in this manuscript, extending and complementing our previous works [11, 12], virtually solve in a straightforward way the problem of the generic error-floor analysis. (No sampling in the configurational space, e.g. of the kind used in [4], was required). We intentionally choose the well known (155, 64, 20) code (used routinely for testing) to demonstrate the exciting opportunities the instanton-amoeba approach has to offer. Our next goal is to apply our scheme to a variety of other (e.g. longer) codes, decoding schemes and channels.

-
- [1] R.G. Gallager, *Low density parity check codes* (MIT Press, Cambridge, 1963).
 - [2] D.J.C. MacKay, *IEEE IT* **45**, 399 (1999).
 - [3] C. Berrou, A. Glavieux, P. Thitimajshima, Proceedings IEEE International Conference on Communications, 23–26 May 1993, Geneva, Switzerland; vol. 2, pp. 1064–70.
 - [4] T. Richardson, *Error floors of LDPC codes*, 2003 Allerton conference Proceedings.
 - [5] N. Wiberg, *Codes and decoding on general graphs*, Ph.D. thesis, Linköping University, 1996.
 - [6] G.D. Forney Jr., R. Koetter, F.R. Kschischang, A. Reznik, *IMA Volumes in Mathematics and its Applications* **123**, 101 (2001).
 - [7] S. Benedetto, G. Montorsi, *IEEE IT* **42**, 409 (1996).
 - [8] Y. Mao, A.H. Banihashemi, *Proc. IEEE Int. Conf. Communications* **1**, 41 (2001).
 - [9] C. Di, D. Proietti, I.E. Telatar, T.J. Richardson, R.L. Urbanke, *IEEE IT* **48**, 1570 (2002).
 - [10] P.O. Vontobel, R. Koetter, Proceedings of IEEE International Symposium on Information Theory, Chicago, IL, Jun./Jul. 2004, p.70.
 - [11] M.G. Stepanov, V. Chernyak, M. Chertkov, B. Vasic, *Diagnosis of weaknesses in modern error correction codes: a physics approach*, <http://arxiv.org/abs/cond-mat/0506037> .
 - [12] V. Chernyak, M. Chertkov, M.G. Stepanov, B. Vasic, *Phys. Rev. Lett.* **93**, 198702 (2004).
 - [13] W.H. Press *et al.* *Numerical recipes in C: the art of scientific computing* (Cambridge University Press, 1988).
 - [14] R.M. Tanner, D. Srkdhara, T. Fuja, Proc. of ICSTA 2001, Ambleside, England.
 - [15] G.P. Agrawal, *Fiber Optic Communication Systems* (Wiley, New York 1997).
 - [16] H.A. Bethe, Proc. Roy. Soc. London A **150**, 552 (1935).